J|A|C|S
ARTICLES
Published on Web 01/31/2006

The 2,6-Diisocyanoazulene Motif: Synthesis and Efficient Mono- and Heterobimetallic Complexation with Controlled Orientation of the Azulenic Dipole

Thomas C. Holovics, Randall E. Robinson, Edward C. Weintrob, Masaharu Toriyama,† Gerald H. Lushington, and Mikhail V. Barybin*

Contribution from the Department of Chemistry, The University of Kansas, 1251 Wescoe Hall Drive, Lawrence, Kansas 66045

Received June 14, 2005; Revised Manuscript Received January 4, 2006; E-mail: mbarybin@ku.edu

Abstract: Synthesis of the remarkably air- and thermally stable 2,6-diisocyano-1,3-diethoxycarbonylazulene linker from 2-amino-1,3-diethoxycarbonylazulene in 57% cumulative yield was developed. Incorporation of the ester "arms" in the design of this first diisocyanoazulene bridge permitted fully controlled stepwise installation and complexation of its isocyano junction groups. The $-CO_2Et$ arms in 2,6-diformamido-1,3-diethoxycarbonylazulene effectively suppress the rate of dehydration of its 2-NHCHO end relative to that of the 6-NHCHO end leading to practically exclusive formation of 6-isocyano-2-formamido-1,3-diethoxycarbonylazulene upon treatment of the above diformamide with an equimolar amount of $POCl_3$. This crystallographically characterized 6-isocyano-2-formamidoazulene derivative was employed to access mono- and heterobimetallic complexes of the 2,6-diisocyanoazulene scaffold with controlled orientation of the azulenic dipole. A complete series of monometallic, homobimetallic, and isomeric heterobimetallic ([M] = $M(CO)_5$, M = Cr and/or W) complexes of the 2,6-diisocyanoazulene motif was isolated and studied by a variety of techniques, including X-ray crystallography. The metal-to-bridge charge transfer in mono- and dinuclear adducts of 2,6-diisocyanoazulene, the assignment of which was corroborated by time-dependent density functional theory calculations, occurs at a dramatically lower energy as compared to the analogous systems featuring the 1,4-diisocyanobenzene scaffold. Moreover, the metal-to-diisocyanide charge transfer exhibits a substantially greater red shift upon binucleation of the mononuclear $[M(CO)_5]$ adducts of the nonbenzenoid 2,6-diisocyanoazulene linker versus the 1,4-diisocyanobenzene bridge.

Introduction

Azulene (bicyclo[5.3.0]decapentaene, Figure 1a) is an azure-blue, polar ($p_e = 1.08$ D[1]), nonbenzenoid hydrocarbon with the aromatic delocalization energy ca. 5 times lower than that of benzene.[2] Being markedly different from those of benzenoid aromatics, the physicochemical characteristics of this highly polarizable "molecular diode" have been used in developing novel advanced organic materials, including nonlinear chromophores,[3] conducting polymers,[4] optoelectronic molecular switches,[5] liquid crystals,[6] anion receptors/sensors,[7] and highly conductive charge-transfer complexes.[8] However, the azulenic scaffold has rarely been employed in the design of functional organometallic systems,[9] and its use as a supramolecular building block in coordination chemistry is virtually unexplored. Despite intriguing theoretical studies on 2,6-azulene-bridged reservoirs,[10] experimental realization of such frameworks is exceedingly scarce[11,12] and has likely been hampered by a high propensity of the azulenic moiety to undergo multi-hapto (and often poorly predictable)[13] coordination to metal atoms/ions, as

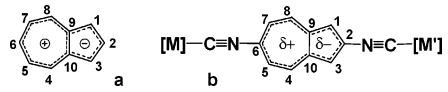

Figure 1. (a) The resonance form of azulene emphasizing its polar nature; (b) hitherto unknown bridging 2,6-diisocyanoazulene motif.

† On sabbatical leave from Nihon University, Japan.

(1) Anderson, A. G.; Steckler, B. M. *J. Am. Chem. Soc.* **1959**, *81*, 4941−4946.
(2) Dewar, M. J. S. *The Molecular Orbital Theory of Organic Chemistry*; McGraw-Hill: New York, 1969.
(3) For example: (a) Liu, R. S. H.; Asato, A. E. *J. Photochem. Photobiol. C* **2003**, *4*, 179−194. (b) Lacroix, P. G.; Malfant, I.; Iftime, G.; Razus, A. C.; Nakatani, K.; Delaire, J. A. *Chem.—Eur. J.* **2000**, *6*, 2599−2608 and references therein. (c) Iftime, G.; Lacroix, P. G.; Nakatani, K.; Razus, A. C. *Tetrahedron Lett.* **1998**, 6853−6856.
(4) Selected examples: (a) Wang, F.; Lai, Y.-H.; Han, M. Y. *Macromolecules* **2004**, *37*, 3222−3230. (b) Redl, F. X.; Köthe, O.; Röckl, K.; Bauer, W.; Daub, J. *Macromol. Chem. Phys.* **2000**, *201*, 2091−2100.
(5) Feringa, B. L.; van Delden, R. A.; Koumura, N.; Geertsema, E. M. *Chem. Rev.* **2000**, *100*, 1789−1816.
(6) (a) Ito, S.; Inabe, H.; Morita, N.; Ohta, K.; Kitamura, T.; Imafuku, K. *J. Am. Chem. Soc.* **2003**, *125*, 1669−1680. (b) Estdale, S. E.; Brettle, R.; Dunmur, D. A.; Marson, C. M. *J. Mater. Chem.* **1997**, *7*, 391−401.
(7) (a) Salman, H.; Abraham, Y.; Tal, S.; Meltzman, S.; Kapon, M.; Tessler, N.; Speiser, S.; Eichen, Y. *Eur. J. Org. Chem.* **2005**, 2207−2212. (b) Zielinski, T.; Kedziorek, M.; Jurczak, J. *Tetrahedron Lett.* **2005**, *46*, 6231−6234.
(8) Schmitt, S.; Baumgarten, M.; Simon, J.; Hafner, K. *Angew. Chem., Int. Ed.* **1998**, *37*, 1077−1081.
(9) Selected examples: (a) Colby, D. A.; Ferrence, G. M.; Lash, T. D. *Angew. Chem., Int. Ed.* **2004**, *43*, 1346−1349. (b) Yeow, E. K. L.; Ziolek, M.; Karolczak, J.; Shevyakov, S. V.; Asato, A. E.; Maciejewski, A.; Steer, R. P. *J. Phys. Chem. A* **2004**, *108*, 10980−10988. (c) Wang, F.; Lai, Y. H.; Han, M. Y. *Org. Lett.* **2003**, *5*, 4791−4794. (d) Farrell, T.; et al. *J. Chem. Soc., Dalton Trans.* **2001**, 29−36. (e) Herrmann, R.; Pedersen, B.; Wagner, G.; Youn, J.-H. *J. Organomet. Chem.* **1998**, *571*, 261−266.
(10) Treboux, G.; Lapstun, P.; Silverbrook, K. *J. Phys. Chem. B* **1998**, *102*, 8978−8980.

10.1021/ja053933+ CCC: $33.50

well as a limited availability of 2,6-functionalized azulenes. Very recently, Chisholm, Dalal, Barybin, and co-workers have shown that the π^*-system of 2,6-azulenedicarboxylate is exceptionally efficient in mediating long-range electronic coupling of metal−metal quadruple bonds.[11]

Aromatic diisocyanides (e.g., 1,4-CN−C_6H_4−NC) continue to be the subject of intense investigations as building blocks in coordination[14] and surface[14a,15] chemistry and as charge-transport mediators[16] for possible applications in nanotechnology. 1,4-Diisocyanobenzene, diisocyanodurene (1,4-CN−C_6Me_4−NC), 1,4-diisocyanonaphthalene, 9,10-diisocyanoanthracene, and 4,4′-diisocyanobiphenyl are by far the most studied aryl diisocyanides in this regard.[14−16] Aryl diisocyanides exhibit lower barriers to conduction as compared to the aryl dithiol congeners thereof, and the lowest barriers to electron transfer appear to occur in the systems where M(dπ) → bridge(pπ^*) interaction can take place (e.g., M = Pd^0).[15c,16c] With the exception of 1,1′-diisocyanoferrocene,[17] all aromatic diisocyanides currently known possess benzenoid π-systems.

Given the unusual nature of the nonbenzenoid azulenic scaffold,[18] we have initiated systematic studies of the rigid linear 2,6-diisocyanoazulene motif (Figure 1b) as an alternative to the customarily employed 1,4-diisocyanobenzene-based linker.[14−16] The asymmetric nature of this hitherto unknown bridge poses a considerable synthetic challenge when [M] ≠ [M′] in Figure 1b, if controlled orientation of the azulenic dipole is desired. Recently, we have described all five possible isocyanoazulenes and shown that up to six azulenyl groups can be electronically coupled to a low-valent metal center via isocyano links.[19] Herein, we report on the synthesis of the first 2,6-diisocyanoazulene bridge and demonstrate a conceptually new, highly regioselective strategy for stepwise installation and complexation of its NC junction groups.

Scheme 1. Synthesis of the 2,6-Diisocyanoazulene Derivative **6**[a]

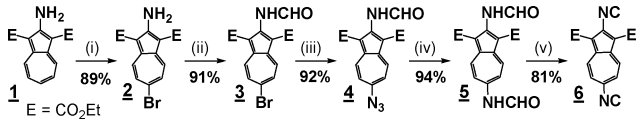

[a] (i) Br_2, 0 °C; (ii) HC(O)OAc, RT; (iii) NaN_3, 70 °C; (iv) $FeCl_3$/NaI/MeCN, then HC(O)OAc, RT; (v) ex. $POCl_3$, RT.

Table 1. IR and ^{13}C NMR Signatures of Isocyano Groups in **6**−**12**[a]

	$\delta(^{13}CN)$, ppm[b]	ν_{CN}, cm^{-1} [c]
6-CN−$C_{10}H_4$−1,3-$(CO_2Et)_2$[d]	168.1	2115
2-CN−$C_{10}H_4$−1,3-$(CO_2Et)_2$[d]	177.5	2127
6	170.1, *179.9*	2116, *2125*
7a	181.5, *185.8*	2123, *2135*
7b	161.1, *165.9*	2123, *2136*
8a	169.7, *186.6*	2115, *2135*
8b	169.9, 165.9	2114, *2135*
9a	182.0, *179.3*	2125, *2125*
9b	161.4, *179.5*	2124, *2124*
10	167.7	2116
11	178.3	2125
12a	181.8, *165.8*	2123, *2135*
12b	160.8, *186.0*	2125, *2133*

[a] Plain and italicized entries refer to 6-isocyano and 2-isocyano groups, respectively. [b] In $CDCl_3$. [c] In CH_2Cl_2. [d] Reference 23.

Results and Discussion

Synthesis of the 2,6-Diisocyanoazulene Framework. The synthesis of a 1,3-substituted 2,6-diisocyanoazulene from 2-amino-1,3-diethoxycarbonylazulene, **1**, in a 57% cumulative yield is summarized in Scheme 1. After bromination of **1** exclusively at position 6,[20] the azulenic moiety was activated toward nucleophilic substitution by converting amine **2** into formamide **3**. Treatment of **3** with NaN_3 gave azide **4**. Notably, attempts to install the 6-azido group by combining **2** with sodium azide invariably led to recovery of the starting materials. The above lack of reactivity of **2** toward N_3^- may be explained by the electron-donating nature of the 2-amino group in **2**, which inhibits nucleophilic substitution of the 6-Br substituent. Among many reductants considered, only the unusual system $FeCl_3$/NaI/MeCN[21] effected clean reduction of the azido functionality of **4**. Without isolation, the reduction product was formylated to provide diformamide **5**, double dehydration of which afforded diisocyanide **6** as lavender leaflets.

Unlike many benzenoid aryl isocyanides,[22] **6** is remarkably air- and thermally stable and can be stored in air at ambient temperature for months without detectable deterioration. The ν_{CN} and $\delta(^{13}CN)$ characteristics of the 2- and 6-isocyano groups in **6** nicely parallel those recorded for the −NC substituents in the corresponding monoisocyano-1,3-diethoxycarbonylazulenes[23] (Table 1). The ^{13}C NMR resonance for the 6-N*C* terminal carbon atom in **6** is 10 ppm shielded compared to that observed for the 2-N*C* carbon. Also, the stretching frequency of the 6-NC group in **6** is 9 cm^{-1} lower than that of the 2-NC oscillator. These differences suggest a slightly reduced C−N bond order within the 6-NC group relative to the 2-NC group in **6**. For

(11) For a recent report on the 2,6-azulenedicarboxylate bridge, see: Barybin, M. V.; Chisholm, M. H.; Dalal, N. S.; Holovics, T. H.; Patmore, N. J.; Robinson, R. E.; Zipse, D. J. *J. Am. Chem. Soc.* **2005**, *127*, 15182−15190.
(12) Lambert, C.; Nöll, G.; Zabel, M.; Hampel, F.; Schmälzlin, E.; Bräuchle, C.; Meerholz, K. *Chem.—Eur. J.* **2003**, *9*, 4232−4239.
(13) Selected examples: (a) Töfke, S.; Behrens, U. *Angew. Chem., Int. Ed. Engl.* **1987**, *26*, 147−148. (b) Churchill, M. R. *Prog. Inorg. Chem.* **1970**, *11*, 53−98. (c) Fedushkin, I. L.; Bochkarev, M. N.; Mühle, S.; Schumann, H. *Russ. Chem. Bull., Int. Ed.* **2003**, *52*, 2005−2011.
(14) For example: (a) Siemeling, U.; et al. *J. Am. Chem. Soc.* **2005**, *127*, 1102−1103. (b) Holliday, B. J.; Farrell, J. R.; Mirkin, C. A. *J. Am. Chem. Soc.* **1999**, *121*, 6316−6317. (c) Yang, L.; Cheung, K.-K.; Mayr, A. *J. Organomet. Chem.* **1999**, *585*, 26−34. (d) Irwin, M. J.; Jia, G. C.; Vittal, J. J.; Puddephatt, R. J. *Organometallics* **1996**, *15*, 5321−5329.
(15) Recent examples: (a) Pranger, L.; Goldstein, A.; Tannenbaum, R. *Langmuir* **2005**, *21*, 5396−5404. (b) Swanson, S. A.; McClain, R.; Lovejoy, K. S.; Alamdari, N. B.; Hamilton, J. S.; Scott, J. C. *Langmuir* **2005**, *21*, 5034−5039. (c) Murphy, K. L.; Tysoe, W. T.; Bennett, D. W. *Langmuir* **2004**, *20*, 1732−1738. (c) Ansell, M. A.; Cogan, E. B.; Page, C. J. *Langmuir* **2000**, *16*, 1172−1179. (d) Henderson, J. I.; Feng, S.; Bein, T.; Kubiak, C. P. *Langmuir* **2000**, *16*, 6183−6187. (e) Ontko, A. C.; Angelici, R. J. *Langmuir* **1998**, *14*, 3071−3078.
(16) (a) McCreery, R. L. *Chem. Mater.* **2004**, *16*, 4477−4496. (b) Chen, J.; et al. *Ann. NY Acad. Sci.* **2002**, *960*, 69−99. (c) Hong, S.; Reifenberger, R.; Tian, W.; Datta, S.; Henderson, J.; Kubiak, C. P. *Superlattices Microstruct.* **2000**, *28*, 289−303. (d) Hanack, M.; Kamenzin, S.; Kamenzin, C.; Subramanian, L. R. *Synth. Met.* **2000**, *110*, 93−103. (e) Seminario, J. M.; Zacarias, A. G.; Tour, J. M. *J. Am. Chem. Soc.* **1999**, *121*, 411−416. (f) Chen, J.; Calvet, L. C.; Reed, M. A.; Carr, D. W.; Grubisha, D. S.; Bennett, D. W. *Chem. Phys. Lett.* **1999**, *313*, 741−748.
(17) Van Leusen, D.; Hessen, B. *Organometallics* **2001**, *20*, 224−226.
(18) (a) Hansen, H. J. *Chimia* **1997**, *51*, 147−159. (b) Hansen, H. J. *Chimia* **1996**, *50*, 489−496. (c) Heilbronner, E. In *Non-Benzenoid Aromatic Compounds*; Ginsburg, D., Ed.; Interscience Publishers: New York, 1959; pp 171−276. (d) Lloyd, D. *Non-Benzenoid Conjugated Carbocyclic Compounds*; Elsevier: New York, 1984; pp 351−377.
(19) (a) Robinson, R. E.; Holovics, T. C.; Deplazes, S. F.; Powell, D. R.; Lushington, G. H.; Thompson, W. H.; Barybin, M. V. *Organometallics* **2005**, *24*, 2386−2397. (b) Robinson, R. E.; Holovics, T. C.; Deplazes, S. F.; Lushington, G. H.; Powell, D. R.; Barybin, M. V. *J. Am. Chem. Soc.* **2003**, *125*, 4432−4433.
(20) Nozoe, T.; Seto, H.; Matsumura, S. Patent JP 34002977, 1959.
(21) See, for example: Kamal, A.; Ramana, K. V.; Ankati, H. B.; Ramana, A. V. *Tetrahedron Lett.* **2002**, *43*, 6861−6863.
(22) (a) Malatesta, L. *Prog. Inorg. Chem.* **1959**, *1*, 283−379. (b) Ugi, I. *Isonitrile Chemistry*; Academic Press: New York, 1971. (c) Meier, M.; Mueller, B.; Ruechardt, C. *J. Org. Chem.* **1987**, *52*, 648−652.
(23) Dubose, D. L.; Robinson, R. E.; Holovics, T. C.; Moody, D.; Weintrob, E. C.; Berrie, C. L.; Barybin, M. V. Submitted.

Figure 2. Interaction of the 6-NC substituent in **6** with the azulenic moiety.

aryl isocyanides, interaction of the −NC substituent with the aromatic ring can be described in resonance terms by the structure: $C{=}N^{+}{=}Ar^{-}$ (Ar = aryl).[22a,24] For **6**, such an interaction would be somewhat more favorable in the case of the 6-NC end because disruption of aromaticity of the azulenic nucleus would be partially compensated by aromatization of the five-membered ring, as illustrated in Figure 2. In addition, σ inductive influence of the azulenic dipole should also contribute to slight weakening of the 6-N≡C bond relative to the 2-N≡C bond in **6**.

The electronic absorption spectrum of **6** in CH_2Cl_2 exhibits a broad band (Figure S1) in the visible region with $\lambda_{max} \approx 535$ nm ($\epsilon = 765\ M^{-1}\ cm^{-1}$). This transition corresponds to the HOMO → LUMO (HOMO = Highest Occupied Molecular Orbital, LUMO = Lowest Unoccupied Molecular Orbital) excitation of **6**, which for unsubstituted azulene occurs at $\lambda_{max} = 576$ nm ($^1A \rightarrow {}^1L_b$) in the same solvent. The hypsochromic (blue) shift of this band for **6** relative to azulene is primarily a consequence of inductive stabilization of the HOMO due to the presence of the electron-withdrawing ester groups at the odd (1 and 3) sites of the azulenic nucleus.[18c,25] As we have recently shown both experimentally and theoretically, the effects of the isocyano substituents at positions 2 and 6 on the HOMO−LUMO gap of azulene are relatively small and have mutually opposite signs, thereby partially canceling each other.[19a]

Monometallic and Homobimetallic Complexation of 6. Addition of 2 equiv of in situ-generated[26] $Cr(CO)_5$(THF) or $W(CO)_5$(THF) to **6** yielded its binuclear adducts **7a** or **7b**, respectively, in nearly quantitative yields. Since the lone pair of the terminal carbon atom of an isocyanide ligand is somewhat antibonding in the C≡N region, the difference between ν_{CN} values for the free and complexed isocyanides may be positive or negative depending on the relative contributions of RNC(σ) → M and M(dπ) → CNR(pπ^*) interactions to the synergistic character of the M−CNR bond.[24] The C−N stretching frequencies for both isocyano groups in **6** undergo ca. 10 cm^{-1} shifts to higher energy upon binding to the zero-valent $M(CO)_5$ (M = Cr or W) units, therefore, indicating dominant (but not exclusive) influence of the RNC(σ) → M interaction on ν_{CN} observed for **7a**/**b** (Table 1). In contrast, the ν_{CN} value for $[Cr(CO)_5]_2$(μ-CNfcNC) (CNfcNC = 1,1′-diisocyanoferrocene), the only other $[Cr(CO)_5]_2$(μ-diisocyanide) species reported,[14a] is 24 cm^{-1} greater than that for free CNfcNC, which suggests lower σ-donor/π-acceptor ratio[24] of **6** as a ligand compared to that of CNfcNC.

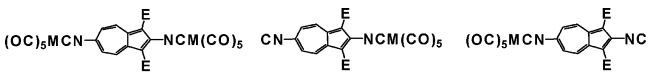

M = Cr: **7a** M = W: **7b** M = Cr: **8a** M = W: **8b** M = Cr: **9a** M = W: **9b**

Upon going from **7a** to **7b**, there is a 20 ppm increase in shielding of $\delta(^{13}C)$ for all carbon atoms within the $[(OC)_5M(CN)]$ units (Tables 1 and 2). This phenomenon, known as the "metal triad ^{13}C shielding trend", is due in part to the increase in the diamagnetic shielding term of the ligand's ^{13}C chemical shift with increasing size of the metal.[27a] The 10 ppm difference between the $\delta(^{13}C)$ values for the two isocyano carbon atoms in **6** shrinks by a factor of 2 upon dinuclear complexation of **6** to give **7a** or **7b** (Table 1). This can be traced to slightly stronger π-acceptor and/or weaker σ-donor character of the 6-NC end of the bridge as compared to its 2-NC end. The marginally greater *net* donor ability of the 2-NC end of **6** is also reflected by the fact that, for both **7a** and **7b**, the ^{13}C resonances for the "$M(CO)_5$" unit attached to the 2-NC junction are slightly deshielded (stronger M(dπ) → CO(pπ^*) back-bonding)[27b,c] with respect to the corresponding resonances for the "$M(CO)_5$" fragment bound to the 6-NC group (Table 2). The above ^{13}C NMR observations are in accord with our quantitative electrochemical demonstration of somewhat higher donor/acceptor ratio of 2-isocyanoazulene than that of 6-isocyanoazulene.[19]

Table 2. ^{13}C NMR Signatures of Carbonyl Ligands in **7**, **8**, **9**, **11**, and **12**[a]

	δ(*trans*-^{13}CO), ppm[b]	δ(*cis*-^{13}CO), ppm[c]
7a	215.4, *216.5*	213.8, *214.5*
7b	195.0, *196.2*	193.4, *194.0*
8a	216.3	214.4
8b	196.1	194.0
9a	215.3	214.1
9b	195.0	193.3
12a	215.3, *196.2*	213.8, *194.0*
12b	195.1, *216.4*	193.4, *214.4*

[a] Plain and italicized entries refer to the $M(CO)_5$ units attached to 6-isocyano and 2-isocyano groups, respectively. [b] CO trans to the isocyanide ligand. [c] CO's cis to the isocyanide ligand.

Treatment of **6** with 1/2 equiv of $Cr(CO)_5$(THF) produced (along with unconsumed **6**) violet **7a** ($R_f = 0.79$) and two blood red mononuclear complexes **8a** ($R_f = 0.53$) and **9a** ($R_f = 0.39$), all of which were easily separated by flash chromatography on SiO_2 using neat CH_2Cl_2. The chromium complexes **7a**, **8a**, and **9a** formed in a 1:2:2 ratio, indicating complete lack of regioselectivity of complexation. However, when a solution of 1/2 equiv of $W(CO)_5$(THF) had been slowly combined with that of **6**, magenta-colored dinuclear **7b** and orange−red mononuclear **8b** and **9b** were obtained reproducibly in a surprising 1:2:1 ratio. This suggests preference, albeit mediocre, in complexation of the apparently more hindered 2-isocyano end of **6**, which has a marginally stronger *net* donor character. For either Cr or W systems, no isomerization of **8** into **9** or vice versa was detected even upon prolonged (>1 day) refluxing of the individual isomers in THF, a fact consistent with kinetic control of the interaction of the diisocyanoazulene with $M(CO)_5$(THF).

Given that mononuclear chromium complexes **8a** and **9a** constitute hybrids of **6** and **7a**, differentiation between isomers **8a** and **9a** based on their ν_{CN} and $\delta(^{13}CN)$ values proved straightforward (Table 1) and was further confirmed via crystallographic characterization of **8a**, as well as an independent

(24) Treichel, P. M. *Adv. Organomet. Chem.* **1973**, *11*, 21−86.
(25) Shevyakov, S. V.; Li, H.; Muthyala, R.; Asato, A. E.; Croney, J. C.; Jameson, D. M.; Liu, R. S. H. *J. Phys. Chem. A* **2003**, *107*, 3295−3299.
(26) Herrmann, W. A.; Zybill, C. In *Synthetic Methods of Organometallic and Inorganic Chemistry (Herrmann/Brauer)*; Herrmann, W. A., Salzer, A., Eds.; Thieme: Stuttgart, 1996; Vol. 1, pp 117−119.
(27) (a) Cronin, D. L.; Wilkinson, J. R.; Todd, L. J. *J. Magn. Reson.* **1975**, *17*, 353−361. (b) Drago, R. S. *Physical Methods in Chemistry*; Surfside Scientific Publishers: Gainesville, FL, 1992; Chapter 8, p 323. (c) Gansow, O. A.; Kimura, B. Y.; Dobson, G. R.; Brown, R. A. *J. Am. Chem. Soc.* **1971**, *93*, 5922−5924.

Scheme 2. Controlled Mono- and Heterobimetallic Complexation of **6**[a]

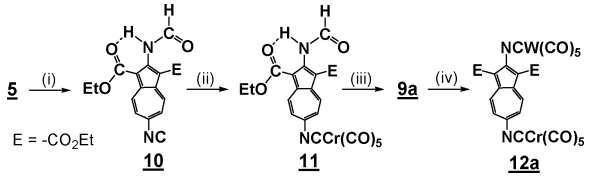

[a] (i) 1.0 equiv of $POCl_3$, 0 °C; (ii) $Cr(CO)_5(THF)$, RT; (iii) $POCl_3$, RT; (iv) $W(CO)_5(THF)$, RT.

synthesis of **9a** (vide infra). The tungsten species **7b**, **8b**, and **9b** have physical (e.g., R_f, melting point) and ν_{CN} properties very similar to those of the corresponding chromium congeners. The ester "arms" in the structure of **6** ensure good solubility of its dinuclear adducts **7** in common polar organic solvents. On the contrary, $[(OC)_5W]_2(\mu\text{-}1,4\text{-}CNC_6H_4NC)$ is practically insoluble in such media.[28] The air and thermal stability of all **7**, **8**, and **9**, as well as their excellent tolerability of chromatographic silica, are remarkable. Notably, the benzenoid analogues $[(OC)_5Cr]_x(1,4\text{-}CNC_6Me_4NC)$ ($x = 1$ or 2) of **7a** and **8a**/**9a** proved moderately air-sensitive (especially in solution) and decomposed extensively upon exposure to silica or neutral alumina.[29]

Regiospecific Monometallic and Heterobimetallic Complexation of 6. If applied to the 2,6-diisocyanoazulene motif, the conventional approach for heterobimetallic complexation of diisocyanides via mononuclear intermediates[30] would (1) require using an excess of the valuable azulenic linker and (2) be compromised by the asymmetric nature of the azulenic moiety. Thus, developing a strategy for *controlled stepwise* complexation of the 2,6-diisocyanoazulene building block constitutes an important synthetic challenge.

Incorporation of two ester arms into the design of the 2,6-diisocyanoazulene linker stemmed, in part, from our earlier serendipitous discovery that dehydration of 2- or 6-formamidoazulenes had occurred much faster than that of 2-formamido-1,3-diethoxycarbonylazulene.[19,29] Gratifyingly, when 1.0 equiv of $POCl_3$ had been slowly added to diformamide **5** in CH_2Cl_2 at 0 °C, 2-formamido-6-isocyanoazulene (**10**) was produced in 70% yield, which approached quantitative if corrected for unconsumed **5** (Scheme 2).[31] Remarkably, only a nonisolable trace of diisocyanide **6** was observed in the above reaction mixture by TLC, and no 6-formamido-2-isocyano isomer of **10** was detected at all. Hence, the $-CO_2Et$ arms in **5** effectively suppress the rate of dehydration of its 2-NHCHO end *relative* to that of the 6-NHCHO end. The transformation **5** → **10** is the first example of highly regiospecific monodehydration of an organic bis(formamide), to the best of our knowledge.

The ν_{CN} and $\delta(^{13}C)$ signatures of the 6-isocyano group in **10** are very similar to the corresponding values documented for the 6-NC substituent in diisocyanide **6** (Table 1). Interestingly, while *N*-monosubstituted formamides, including 2-formamidoazulene,[19a] usually exist in solution as equilibrium mixtures of two conformational isomers due to hindered rotation about the OHC−NHR bond,[32] the ^1H and ^{13}C NMR spectra of **10** in CD_2Cl_2 or $CDCl_3$ feature only one set of resonances. The very small $^3J_{HH}$ coupling constant (<2 Hz) observed for the formamido moiety of **10** is consistent with *cis* disposition of the C−H and N−H bonds (hence, *trans* orientation of the C═O and N−H bonds) with respect to the partially double OHC−NHR bond (Scheme 2). This is the thermodynamically preferred geometry of a formamide.[33] Notably, the NH group of **10** appears to be involved in a hydrogen bonding interaction, most likely intramolecularly with an ester carbonyl, as evidenced by the broad ν_{NH} band at 3286 cm^{-1} in CH_2Cl_2. In contrast, the ν_{NH} bands recorded for 2-formamidoazulene are sharp and occur at 3418 and 3383 cm^{-1} in the same solvent.[19a] Favorability of internal hydrogen bonding in **10** can be attributed to lack of torsional strain upon closing the H-bonded six-membered ring and low entropic barrier to the internal H-bond formation.[34]

The accessibility of **10** allowed us to prepare monometallic and heterobimetallic adducts of **6** in fully controlled fashion according to Scheme 2. Complexation of the isocyano end of **10** with the $Cr(CO)_5$ fragment followed by dehydration of the 2-formamido group in the resulting species **11** afforded mononuclear complex **9a** in ca. 80% cumulative isolated yield. Similar to **10**, formamide **11** exists as a single conformational isomer in CH_2Cl_2 or $CHCl_3$ solutions (Figures S2 and S3). Treatment of **9a** with 1 equiv of $W(CO)_5(THF)$ provided Cr,W-heterobimetallic complex **12a**. The isomer of **12a** that features interchanged positions of the Cr and W centers (compound **12b**) was obtained by switching conditions (ii) and (iv) in Scheme 2. While **12a** and **12b** exhibit superimposable ^1H NMR and FTIR characteristics, they can be easily distinguished on the basis of the $\delta(^{13}C)$ values for their isocyano junction groups, given that these isomers constitute hybrids of homobimetallic **7a** and **7b** (Table 1).

X-ray Crystallographic Studies. The single-crystal X-ray analysis of **7a** (Figure 3, top) revealed that its $[(OC)_5Cr(CN)]$ units have essentially identical metric parameters (Table 3) and feature the Cr−C distances that are statistically shorter (by at least 10 σ) than the corresponding bonds within $[Cr(CO)_5]_2(\mu\text{-}CNfcNC)$.[14a] Thus, the synergistic (i.e., σ-bonding/π-backbonding) Cr−C interactions in **7a** are stronger than those in $[Cr(CO)_5]_2(\mu\text{-}CNfcNC)$. Coupled with the analysis of ν_{CN} for **6**, CNfcNC, and the bis-$[Cr(CO)_5]$ adducts thereof (vide supra), this reflects superior π-accepting capability of **6** with respect to that of CNfcNC. The crystal structures of **7b** (Figure 3), **12a**, and **12b** (Figure 4) are all isomorphous with that of **7a** ($P\bar{1}$, Table S1). In the above series of compounds, the W−C bonds are 0.13−0.15 Å longer than the Cr−C bonds (Table 3). Consequently, the M···M separation varies in the order **7a** (13.95 Å) < **12b** (14.09 Å) ≈ **12a** (14.10 Å) < **7b** (14.23 Å). Notably, both carboxylate moieties in **7a**/**b** and **12a**/**b** are coplanar with the azulenic framework, and the −OEt arms embrace the 2-NC junction (Figures 3 and 4).

In **7a/b** and **12a/b**, the C2−N21−C21 and C6−N61−C61 angles exhibit 15° bending *out* of the aromatic plane (Table 3). While distortions of such a magnitude were shown to have minute energetic consequences,[35] this mode of bending at

(28) Rommel, J. S.; Weinrach, J. B.; Grubisha, D. S.; Bennett, D. W. *Inorg. Chem.* **1988**, *27*, 2945−2949.
(29) Holovics, T. C.; Barybin, M. V. Unpublished observations.
(30) Grubisha, D. S.; Rommel, J. S.; Lane, T. M.; Tysoe, W. T.; Bennett, D. W. *Inorg. Chem.* **1992**, *31*, 5022−5027.
(31) Commercial $POCl_3$ (50 μL) was used as received and might have become slightly deactivated by traces of moisture upon handling.
(32) Kessler, H. *Angew. Chem., Int. Ed. Engl.* **1970**, *9*, 219−235.
(33) Schulz, G. E.; Schirman, R. H. *Principles of Protein Structure*; Springer: New York, 1979.
(34) Gellman, S. H.; Dado, G. P.; Liang, G. B.; Adams, B. R. *J. Am. Chem. Soc.* **1991**, *113*, 1164−1173.

Table 3. Selected Bond Distances (Å) and Angles (deg) in the X-ray Structures of **7a**, **7b**, **8a**, **10**, **12a**, and **12b**

	M–C21	M–C61	C21–N21	C61–N61	N21–C2	N61–C6	C2–C21–N21	C6–N61–C61
7a	1.944(3)	1.948(3)	1.165(4)	1.166(4)	1.371(3)	1.393(3)	164.9(3)	164.9(3)
7b	2.093(6)	2.097(6)	1.165(8)	1.151(8)	1.359(7)	1.394(7)	165.5(6)	165.4(7)
8a	1.953(3)		1.166(4)	1.157(4)	1.375(4)	1.410(4)	167.5(3)	177.3(4)
10			1.359(3)	1.144(3)	1.381(2)	1.412(2)	126.6(2)	176.7(2)
12a	2.087(4)	1.957(4)	1.169(6)	1.163(5)	1.369(5)	1.399(5)	164.3(4)	165.2(4)
12b	1.950(4)	2.088(4)	1.162(5)	1.164(5)	1.373(5)	1.402(5)	163.7(4)	165.6(4)

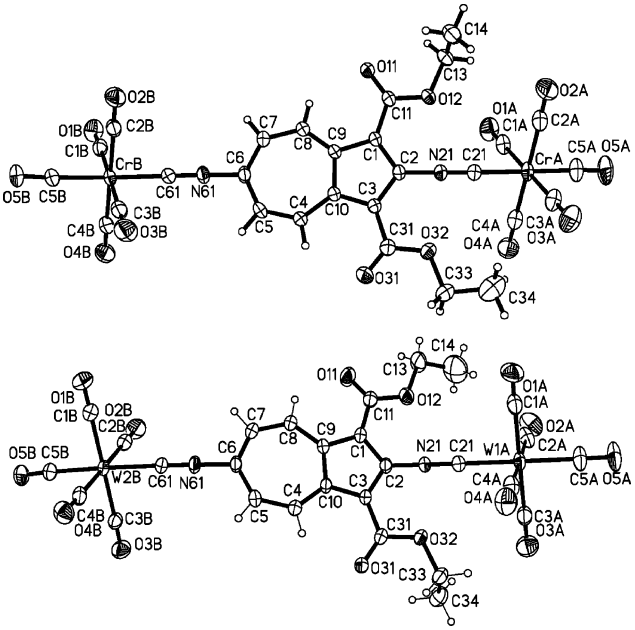

Figure 3. Molecular structures of **7a** (top) and **7b** (bottom), 50% thermal ellipsoids.

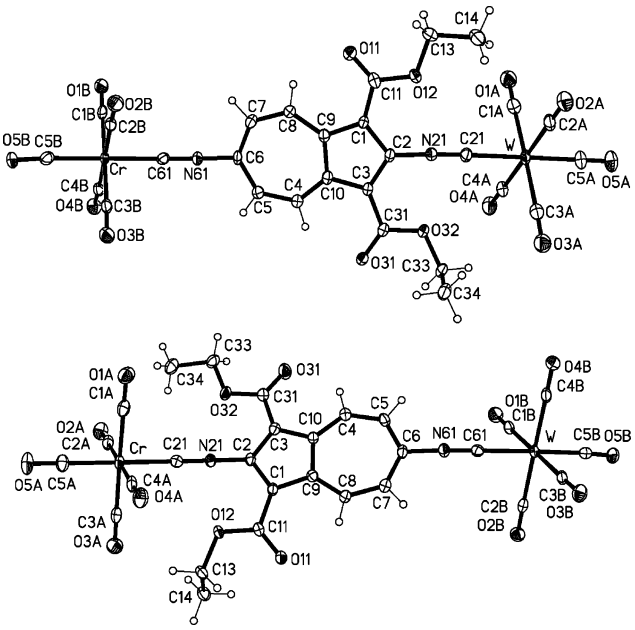

Figure 4. Molecular structures of isomeric **12a** (top) and **12b** (bottom), 50% thermal ellipsoids.

nitrogen is quite different from that observed for $[W(CO)_4(PEt_3)]_2(\mu\text{-}1,4\text{-}CNC_6H_4NC)$.[36] Indeed, the C−N−C bending of 11° documented for $[W(CO)_4(PEt_3)]_2(\mu\text{-}1,4\text{-}CNC_6H_4NC)$ occurs *in* the plane of the bridge and was attributed to substantial M(dπ) → CNR(pπ*) interactions within the complex.[36] It is possible that the *out-of-plane* C−N−C bending in **7a**/**b** and **12a**/**b**

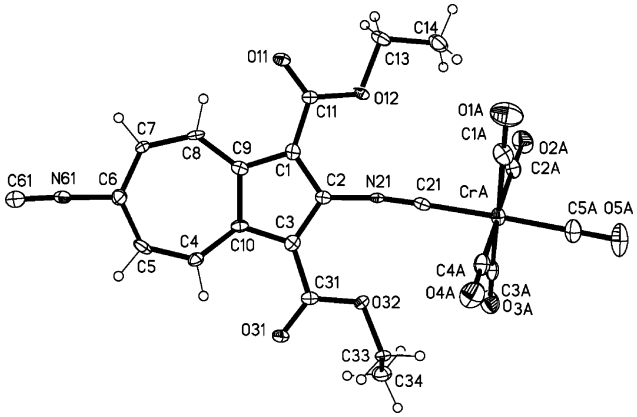

Figure 5. Molecular structure of **8a**, 50% thermal ellipsoids.

happens to enhance σ-donor character[37] of the 2,6-diisocyanoazulene bridge.

The primarily electronic rather than packing origin of the C−N−C bending in **7a/b** and **12a/b** is supported by the fact that the C2−N21−C21 angle in mononuclear **8a**, which features different molecular shape and crystal packing, is very similar in magnitude to the C2−N21−C21 angles in **7a**/**b** and **12a**/**b** (Figure 5, Table 3). Moreover, this C−N−C bending in **8a** also occurs *out* of the aromatic plane. The structural parameters of **8a** nicely parallel those of the corresponding portion in dinuclear **7a**, the only prominent difference being nearly perfect linearity of the uncomplexed C6−N61−C61 unit (Table 3). Compound **8a** crystallizes in the chiral space group *Aba*2. The supramolecular chirality of *achiral* **8a** is confined to the solid state and represents a well-documented, albeit relatively uncommon, crystallographic phenomenon.[38]

The X-ray structure of **10** revealed that its 6-isocyano end is nearly linear, the formamido group assumes the thermodynamically preferred configuration (N−H *trans* to C═O), and the NH unit is hydrogen-bonded to an ester carbonyl (Figure 6, Table 3). The amide hydrogen atom, H21A, was located during refinement. The ester moiety engaged in H-bonding is rotated ca. 180° compared to the orientation of the $-CO_2Et$ arms with respect to the azulenic nucleus in **7a**/**b**, **8a**, or **12a**/**b** (Figures 3−5). The plane of the second ester group forms a ca. 38° angle with the aromatic framework, which is undoubtedly a consequence of steric repulsion between this $-CO_2Et$ group and the −NHCHO end. Thus, the solid-state structural characteristics of **10**, including the intramolecular hydrogen bonding, appear to be preserved in solution (vide supra). A similar H-bonding interaction within diformamide **5** is likely responsible for

(35) Wagner, N. L.; Kloss, J. M.; Murphy, K. L.; Bennett, D. W. *J. Chem. Inf. Comput. Sci.* **2001**, *41*, 50−55.
(36) Rommel, J. S.; Weinrach, J. B.; Grubisha, D. S.; Bennett, D. W. *Inorg. Chem.* **1988**, *27*, 2945−2949.
(37) Bohling, D. A.; Mann, K. R. *Inorg. Chem.* **1984**, *23*, 1426−1432.
(38) Flack, H. D. *Helv. Chim. Acta* **2003**, *86*, 905−921.

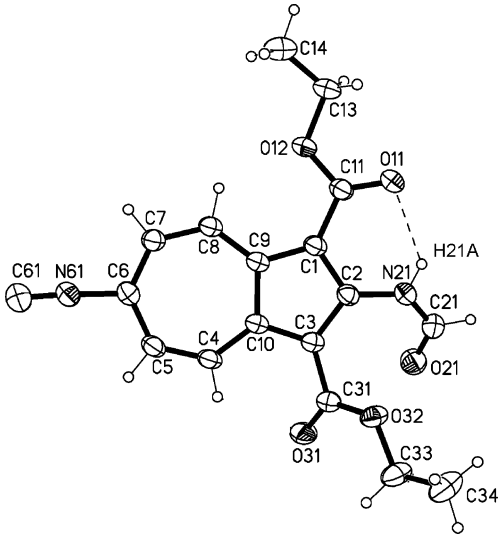

Figure 6. Molecular structure of **10**, 50% thermal ellipsoids. Selected distances (Å) and angles (deg) relevant to H-bonding interaction within **10**: O11···N21 2.736(2), N21−H21A 0.86(3), O11−H21A 2.08(3), N21−H···O11 132.2, torsion C1−C11−O11−H21A 3.5(2).

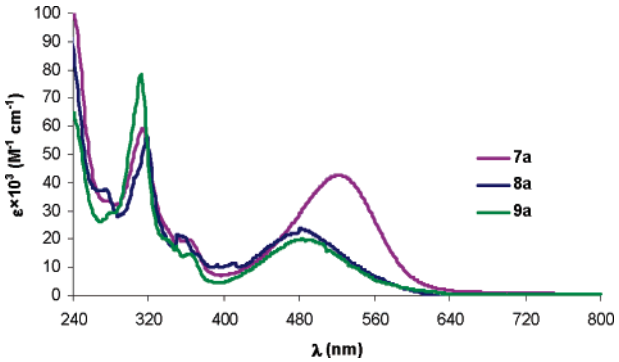

Figure 7. UV−vis spectra of **7a**, **8a**, and **9a** in CH_2Cl_2 at 22 °C.

Table 4. Properties of the MLCT (L = diisocyanoarene) Bands Observed in the Electronic Spectra of **7**, **8**, **9**, and **12**[a]

	λ_{max}, nm	ν_{max}, cm^{-1}	$\epsilon \times 10^3$, M^{-1} cm^{-1}
7a	522	19 157	43
8a	481	20 790	24
9a	480	20 833	20
7b	515	19 417	49
8b	466	21 459	28
9b	466	21 459	32
12a	518	19 305	45
12b	520	19 230	42
$(OC)_5W(\eta^1$-DIB)[b]	354	28 248	not reported
$[(OC)_5W]_2(\eta^1$: η^1-DIB)[b]	370	27 027	not reported

[a] In CH_2Cl_2 at 22 °C. [b] Reference 30, DIB = 1,4-diisocyanobenzene.

stabilization of a conformation that restricts facile access of $POCl_3$ to the 2-formamido end of **5**, which, in turn, translates into the relatively slow dehydration of its 2-formamido substituent.

Metal-to-Ligand Charge Transfer (MLCT, L = 2,6-Diisocyano-1,3-diethoxycarbonylazulene). The MLCT bands for **8a** and **9a** have almost the same λ_{max}, despite the polar nature of the azulenic nucleus, and undergo dramatic red shifts (ca. 1650 cm^{-1}) upon binucleation to form **7a** (Figure 7, Table 4). This suggests involvement of the aromatic π-system in the MLCT for **7a**, **8a**, and **9a**, as well as greater π-delocalization/resonance stabilization in **7a** versus **8a** or **9a**. A similar, albeit

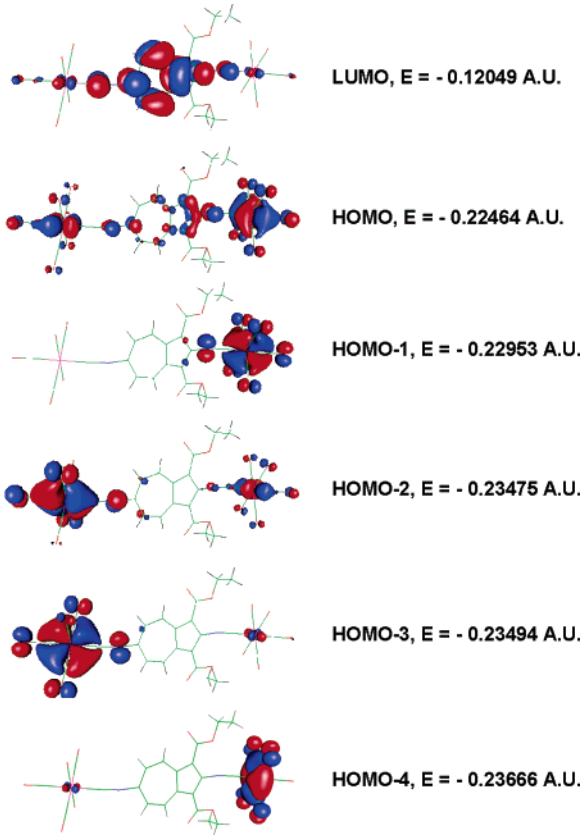

Figure 8. TD-DFT Frontier molecular orbitals of **7a** (solid-state structure).

less pronounced, phenomenon was discovered by Bennett et al. for the binucleation of $(OC)_5W(1,4\text{-}CNC_6H_4NC)$ to give $[(OC)_5W]_2(\mu\text{-}1,4\text{-}CNC_6H_4NC)$.[30]

Our time-dependent density functional theory (TD-DFT) calculations on **7a** confirmed the largely metal-to-bridge charge-transfer character of the lowest energy electronic transition observed for this species. Indeed, the lowest energy TD-DFT excitation with significant oscillator strength predicted for **7a** is described as (0.52 × HOMO + 0.29 × HOMO-3 − 0.31 × HOMO-4) → LUMO, $f = 0.2938$. While the HOMO-3 and HOMO-4 of **7a** are CrB(dπ)- and CrA(dπ)-based, respectively, delocalization within **7a**'s HOMO involves *both* $Cr(CO)_5$ units, as well as the π-system of the linker (Figure 8). The LUMO of **7** is strikingly reminiscent of that of free bridge **6**. Notably, the ester arms do not contribute to any of the Frontier MO's of **7a** shown in Figure 8.

In parallel with their chromium congeners, the tungsten complexes **8b** and **9b** exhibit the MLCT bands of mutually identical energies (Figure 9, Table 4). The red shift of this MLCT transition that occurs upon binucleation of **8b** or **9b** to give **7b** is even more pronounced than that observed for the corresponding Cr systems (Table 5), which may be attributed to greater radial extension (hence better overlap with the linker's π-system) of the W(dπ) versus Cr(dπ) orbitals. As shown in Table 4, the MLCT transfers for **7b**, **8b**, and **9b** are substantially more facile energetically than the MLCT's (L = $1,4\text{-}CNC_6H_4NC$) observed for their corresponding benzenoid analogues $[(OC)_5W]_x$-$(1,4\text{-}CNC_6H_4NC)$ ($x = 1, 2$).[30] This is a consequence of the dramatically reduced aromatic stabilization (and, in turn, lower-lying LUMO) of azulene versus benzene.[2] Moreover, the red shift of the MLCT for the process **8b**/**9b** → **7b** is 820 cm^{-1}

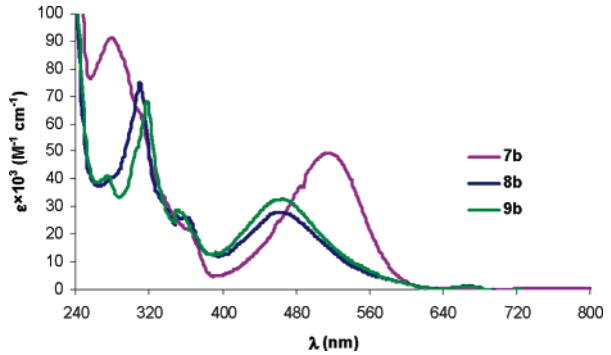

Figure 9. UV−vis spectra of **7b**, **8b**, and **9b** in CH_2Cl_2 at 22 °C.

Table 5. Red Shifts of the MLCT (L = diisocyanoarene) Bands Occurring upon Binucleation of **6** and DIB[a]

binucleation process	ΔE_{MDICT}, cm^{-1}
8a/9a → 7a	≈1650
8b/9b → 7b	2042
$(OC)_5W(\eta^1\text{-DIB}) \rightarrow [(OC)_5W]_2(\eta^1\text{: }\eta^1\text{-DIB})$	1221[b]

[a] DIB = 1,4-diisocyanobenzene. [b] Reference 30.

greater than that reported for the analogous $[(OC)_5W](1,4\text{-}CNC_6H_4NC) \rightarrow [(OC)_5W]_2(1,4\text{-}CNC_6H_4NC)$ binucleation[30] (Table 5). Thus, the 2,6-diisocyanoazulene bridge is more effective than the 1,4-diisocyanoazulene linker in delocalizing π-electrons within the M−bridge−M′ framework. Of note, the electronic spectra of heterobimetallic isomers **12a** and **12b** are virtually superimposable and feature the MLCT bands with λ_{max} values between those recorded for homobimetallic **7a** and **7b** (Figure S4).

Concluding Remarks

(1) The practical synthesis of the first 2,6-diisocyanoazulene derivative **6** described herein, as well as the remarkable stability of this molecule and its metal adducts under ambient conditions, opens new opportunities for the long-overdue exploration of the nonbenzenoid 2,6-azulenic framework as a building block in coordination and surface chemistry.

(2) While the 2,6-diester functionalization of 1,4-diisocyanobenzene is not known and would be difficult to achieve in practice, the topologically analogous 1,3-diester substitution of 2,6-diisocyanoazulene proved straightforward. Such a derivatization of the 2,6-diisocyanoazulene motif ensured convenient solution processibility of its binuclear $[M(CO)_5]$ (M = Cr and/or W) adducts. Moreover, incorporation of the ester arms at 1,3-positions of the azulenic nucleus allowed for the substantial alteration of the relative rates of dehydration of the formamido ends in 2,6-diformamidoazulene. This led to establishing the convenient strategy for highly regioselective installation and complexation of 2,6-diisocyanoazulene's NC junctions. The scope of the above strategy is expected to be quite general, as long as organometallic formamides, such as **11**, tolerate dehydration conditions.

(3) The dipolar nature of the azulenic moiety[1] results in the 2-NC end of **6** having slightly stronger *net* electron-donor character than the 6-NC end, as evidenced by the FTIR and ^{13}C NMR analyses of **6**−**12**. The electronic differences between the two NC junctions are marginal and have virtually no effect on either the M−C bond distances in binuclear **7a**/**b** or the MLCT energies for mononuclear **8a**/**b** versus **9a**/**b**. This is reasonable given that the resonance form of azulene shown in Figure 1a is rather minor as the full ± charge separation within the azulenic framework would have produced the dipole moment of not 1 but 12 D.[11]

(4) Upon binucleation, the π-system of 2,6-diisocyanoazulene provides greater response than that of 1,4-diisocyanobenzene in sensing complexation of one of the NC junctions, which makes the former an attractive alternative to the latter for mediating metal−metal interactions. The metal-to-diisocyanide charge transfers in the mono- and binuclear adducts of the 2,6-diisocyanoazulene motif are exceptionally facile (in context of the diisocyanoarene-linked systems) owing to the much lower aromatic stabilization of the azulenic nucleus as compared to benzenoid frameworks.

Investigations of conductivity properties of the 2,6-diisocyanoazulene scaffold as well as studies encompassing supramolecular, electro-, and surface[23] chemistry of 2,6-diisocyanoazulene-bridged organometallics are in progress.

Experimental Section

General Procedures, Starting Materials, and Equipment. Unless specified otherwise, all operations were performed under an atmosphere of 99.5% argon further purified by passage through columns of activated BASF catalyst and molecular sieves. Standard Schlenk techniques were employed with a double manifold vacuum line. Solvents were freed of impurities by usual procedures and stored under argon. The syntheses of **2**−**5** were conducted under air atmosphere.

Solution infrared spectra were recorded on a Thermo Nicolet Avatar 360 FTIR spectrometer with samples sealed in 0.1 mm gas-tight NaCl cells. NMR samples were analyzed on Bruker DRX-400 and Bruker Avance 500 spectrometers. ^1H and ^{13}C chemical shifts are given with reference to residual ^1H and ^{13}C solvent resonances relative to TMS. Two-dimensional NMR techniques (COSY, HMQC, HMBC) were employed, when necessary, to obtain unambiguous assignments of ^1H and ^{13}C NMR resonances.[39] The aromatic hydrogen resonances are labeled in reference to the corresponding carbon atoms of the azulenic framework (see Figure 1a). UV−vis spectra were recorded in CH_2Cl_2 at 24 °C using a CARY 100 spectrophotometer. Melting points are uncorrected and were determined for samples in sealed capillary tubes. Elemental analyses were carried out by Desert Analytics, Tucson, Arizona. Mass-spectral analyses were performed in the MS laboratory of the University of Kansas.

2-Amino-1,3-diethoxycarbonylazulene,[40] acetic-formic anhydride,[41] and in situ-generated $Cr(CO)_5(THF)$[26] and $W(CO)_5(THF)$[26] were prepared according to literature procedures. Other reagents were obtained from commercial sources. Davisil (200−425 mesh, type 60A) silica gel was used in all chromatographic manipulations.

Synthesis of 2. This procedure is based on that of Nozoe et al.[20] Bromine (3.84 g, 24.0 mmol) was added dropwise to a chilled (0 °C) solution of 2-amino-1,3-diethoxycarbonylazulene (6.90 g, 24.0 mmol) in 250 mL of chloroform with vigorous stirring over a period of 20 min. The ice bath was then removed, and the reaction mixture was allowed to warm to room temperature. After 30 min of stirring at room temperature, formation of an orange precipitate was observed. The mixture was stirred for an additional 30 min period and then poured into 500 mL of distilled water. The organic layer was separated, and the aqueous layer was extracted once with 100 mL of $CHCl_3$. The organic fractions were combined and dried over anhydrous Na_2SO_4. Filtration followed by solvent removal under vacuum provided dark

(39) Levitt, M. H. *Spin Dynamics. Basics of Nuclear Magnetic Resonance*; John Wiley & Sons, LTD: New York, 2001.
(40) Takase, K.; Nozoe, T.; Nakazawa, T.; Fukuda, S. *Tetrahedron* **1971**, *27*, 3357−3368.
(41) Krimen, L. I. *Org. Synth.* **1970**, *50*, 1−3.

orange residue, which was recrystallized from benzene to give orange **2** (7.84 g, 21.4 mmol) in an 89% yield. HRMS (ES, positive *m*/*z*): calcd for $C_{16}H_{17}BrNO_4$ (M + 1), 366.0341; found, 366.0341. ^{1}H NMR (400 MHz, $CDCl_3$, 25 °C): δ 1.47 (t, 3H, CH_3, $^3J_{HH}$ = 7 Hz), 4.45 (q, 2H, CH_2, $^3J_{HH}$ = 7 Hz), 7.77 (d, 2H, $H^{5,7}$, $^3J_{HH}$ = 12 Hz), 8.78 (d, 2H, $H^{4,8}$, $^3J_{HH}$ = 12 Hz) ppm. ^{13}C{^{1}H} NMR (100.6 MHz, $CDCl_3$, 25 °C): δ 14.8 (*C*H_3), 60.3 (*C*H_2), 101.1, 128.5, 129.6, 135.5, 144.4, 162.4 (azulenic C), 166.4 (*C*O_2Et) ppm.

Synthesis of 3. Solid **2** (2.84 g, 7.8 mmol) was treated with excess acetic-formic anhydride (50 mL) and formic acid (10 mL) at room temperature. After stirring the reaction mixture for 3 h, all volatiles were removed under vacuum. The residue was chromatographed on silica gel using the 4:1 $CHCl_3$/Et_2O eluent. A deep red−orange band was collected, which gave crystalline **3** (2.80 g, 7.1 mmol) in a 91% yield after solvent removal and drying at 10^{-2} Torr. Mp 134−138 °C. HRMS (ES, positive *m*/*z*): calcd for $C_{16}H_{17}BrNO_4$ (M + 1), 394.0290; found, 394.0296. ^{1}H NMR (400 MHz, $CDCl_3$, 25 °C): δ 1.47 (t, 3H, CH_3, $^3J_{HH}$ = 7 Hz), 4.47 (q, 2H, CH_2, $^3J_{HH}$ = 7 Hz), 7.99 (d, 2H, $H^{5,7}$, $^3J_{HH}$ = 12 Hz), 8.64 (s, 1H, C*H*O), 9.09 (d, 2H, $H^{4,8}$, $^3J_{HH}$ = 11 Hz), 10.30 (br s, 1H, N*H*) ppm. ^{13}C{^{1}H} NMR (100.6 MHz, $CDCl_3$, 25 °C): δ 14.6 (*C*H_3), 61.3 (*C*H_2), 109.4, 133.9, 134.2, 134.8, 139.9, 147.7 (azulenic C), 165.5 (*C*HO), 166.0 (*C*O_2Et) ppm. Addition of formic acid in this reaction is important to prevent formation of the acetamide analogue of **3**. This acetamide is difficult to separate from **3** by chromatographic means. The acetamide impurity, if generated, will not be detrimental in the subsequent steps, although it will lead to reduction in yield of diisocyanide **6**.

Synthesis of 4. A solution of **3** (5.00 g, 12.7 mmol) and excess sodium azide (4.4 g, 68 mmol) in 200 mL of dry DMSO was heated at 70 °C for 2 h with stirring. Then, the reaction flask was open to air, and the mixture was poured into 1 L of distilled water. The organics were extracted using five 200 mL portions of chloroform. The combined extracts were *thoroughly* washed with water (5 × 100 mL) to remove residual DMSO and dried over anhydrous $MgSO_4$. After filtration, the solvent was removed under vacuum to afford yellow−orange crystalline **4** (4.17 g, 11.7 mmol) in a 92% yield. Mp 124−128 °C (dec). HRMS (ES, positive *m*/*z*): calcd for $C_{16}H_{17}BrNO_4$ (M + 1), 357.1199; found, 357.1202. IR ($CHCl_3$): ν_{NN} 2112 vs; ν_{CO} 1708 m, 1692 m, 1666 m cm^{-1}. ^{1}H NMR (400 MHz, $CDCl_3$, 25 °C): δ 1.46 (t, 3H, CH_3, $^3J_{HH}$ = 7 Hz), 4.46 (q, 2H, CH_2, $^3J_{HH}$ = 7 Hz), 7.29 (d, 2H, $H^{5,7}$, $^3J_{HH}$ = 10 Hz), 8.63 (s, 1H, C*H*O), 9.24 (br d, 2H, $H^{4,8}$, $^3J_{HH}$ ≈ 10 Hz), 10.19 (br s, 1H, N*H*) ppm. ^{13}C{^{1}H} NMR (100.6 MHz, $CDCl_3$, 25 °C): δ 14.6 (*C*H_3), 61.1 (*C*H_2), 109.3, 121.2, 122.1, 135.3, 136.0, 150.1 (azulenic C), 165.6, 166.1 (*C*HO, *C*O_2Et) ppm.

Synthesis of 5. A mixture consisting of **4** (0.725 g, 2.03 mmol), NaI (2.82 g, 18.8 mmol), $FeCl_3(H_2O)_3$ (0.84 g, 3.9 mmol), and acetonitrile (30 mL) was magnetically stirred at room temperature until the very dark slurry formed became too thick to stir. Then, the reaction mixture was poured into 400 mL of $CHCl_3$ and quickly washed with saturated aqueous sodium thiosulfate (2 × 50 mL) and brine (100 mL). The resulting organic solution was dried over Na_2SO_4. After filtration, 350 mL of the solvent was removed under vacuum at $T \leq 25$ °C. Excess acetic-formic anhydride (15 mL) and formic acid (3 mL) were then added to the solution. The mixture was stirred for 2 h, while the progress of the reaction was checked by TLC (4:1 $CHCl_3$/Et_2O). All volatiles were removed under vacuum, and the residue was dried at 10^{-2} Torr to give red−orange **5** (0.681 g, 1.90 mmol) in a 94% yield. Mp: the product decomposed without melting. ^{1}H and ^{13}C NMR spectra of **5** in 10:1 CD_2Cl_2/DMSO feature at least two overlapping sets of signals, presumably due to hindered rotation around the OHC−NHR bond of the 6-NHCHO substituent. While bis(formamide) **5** was used without further purification in the next step, it can be purified by chromatography on silica gel using $CHCl_3$/EtOH (gradual increase of ethanol content up to 20%), if desired.

Synthesis of 6. Excess phosphorus oxychloride (3.30 g, 21.5 mmol) was added to a solution of **5** (1.790 g, 5.00 mmol) and freshly distilled diisopropylamine (20 mL) in 150 mL of CH_2Cl_2 at 20 °C. The reaction mixture was stirred for 1 h after the addition of $POCl_3$ had been completed and then quenched with 200 mL of 10% aqueous K_2CO_3. The aqueous phase was extracted with $CHCl_3$ (2 × 50 mL). The organic fractions were combined and dried over anhydrous $MgSO_4$. Filtration followed by removal of all volatiles on a rotary evaporator afforded a dark lavender residue, which was subject to column chromatography on silica gel using neat $CHCl_3$. A deep lavender band was collected, which gave crystalline **6** (1.306 g, 4.05 mmol) as lavender flakes in an 81% yield after solvent removal and drying at 10^{-2} Torr. Mp: the product decomposed without melting at ca. 250 °C. Anal. Calcd for $C_{18}H_{14}N_2O_4$: C, 67.07; H, 4.38; N, 8.69. Found: C, 67.13; H 4.48; N, 8.95. IR (CH_2Cl_2): ν_{CN} 2125 m, 2116 m; ν_{CO} 1692 s cm^{-1}. ^{1}H NMR (400 MHz, $CDCl_3$, 25 °C): δ 1.52 (t, 3H, CH_3, $^3J_{HH}$ = 7 Hz), 4.53 (q, 2H, CH_2, $^3J_{HH}$ = 7 Hz), 7.79 (d, 2H, $H^{5,7}$, $^3J_{HH}$ = 11 Hz), 9.80 (d, 2H, $H^{4,8}$, $^3J_{HH}$ = 11 Hz) ppm. ^{13}C{^{1}H} NMR (100.6 MHz, $CDCl_3$, 25 °C): δ 14.4 (*C*H_3), 61.8 (*C*H_2), 114.9, 129.2, 132.4, 137.3, 140.0, 140.9 (azulenic C), 163.0 (*C*O_2Et), 170.1 (6-*C*N), 179.9 (2-*C*N) ppm. UV−vis (CH_2Cl_2, λ (log ϵ)): 535 (2.86), 423 (2.79), 408 sh (2.75) nm.

Synthesis of 7a. $Cr(CO)_5$(THF) was generated in situ by photolysis of $Cr(CO)_6$ (0.460 g, 2.09 mmol) dissolved in 200 mL of THF using a Hanovia Hg 450 W immersion lamp. After the formation of $Cr(CO)_5$-(THF) had been judged nearly complete by FTIR in the ν_{CO} region, the resulting red−orange solution was added to a solution of **6** (0.335 g, 1.04 mmol) in 20 mL of THF dropwise via cannula at room temperature. The mixture was stirred for 15 h, while acquiring a dark violet color. Then, the content of the reactor was open to air, and all solvent was removed under vacuum on a rotary evaporator. A minute amount of unreacted $Cr(CO)_6$ was sublimed off (10^{-2} Torr, 40 °C), and the residue was passed through a short silica gel column using neat chloroform. A deep violet band was collected. After solvent removal and drying at 10^{-2} Torr, violet crystalline **7** (0.690 g, 0.98 mmol) was isolated in a 94% yield. Mp 178−180 °C (dec). Anal. Calcd for $C_{28}H_{14}Cr_2N_2O_9$: C, 47.61; H, 2.00; N, 3.97. Found: C, 47.52; H 2.27; N, 4.22. IR (CH_2Cl_2): ν_{CN} 2135 w, 2123 w; ν_{CO} 2028 m, 2048 m, 1968 vs, 1962 vs cm^{-1}. ^{1}H NMR (500 MHz, $CDCl_3$, 25 °C): δ 1.51 (t, 3H, CH_3, $^3J_{HH}$ = 7 Hz), 4.59 (q, 2H, CH_2, $^3J_{HH}$ = 7 Hz), 7.69 (d, 2H, $H^{5,7}$, $^3J_{HH}$ = 11 Hz), 9.75 (d, 2H, $H^{4,8}$, $^3J_{HH}$ = 11 Hz). ^{13}C{^{1}H} NMR (125 MHz, $CDCl_3$, 25 °C): δ 14.9 (*C*H_3), 61.5 (*C*H_2), 114.6, 129.2, 132.5, 137.5, 138.9, 140.9 (azulenic C), 163.1 (*C*O_2Et), 181.5 (6-*C*N), 185.8 (2-*C*N), 213.8 (Cr*C*O, *cis*), 214.5 (Cr*C*O, *cis*), 215.4 (Cr*C*O, *trans*), 216.5 (Cr*C*O, *trans*) ppm.

Synthesis of 7b. Substitution of $W(CO)_6$ for $Cr(CO)_6$ in the above procedure for the synthesis of **7a** provided dark magenta **7b**. Mp 186−188 °C (dec). Anal. Calcd for $C_{28}H_{14}N_2O_{14}W_2$: C, 34.67; H, 1.45; N, 2.89. Found: C, 34.80; H 1.68; N, 2.96. IR (CH_2Cl_2): ν_{CN} 2136 w, 2123 w; ν_{CO} 2028 m, 2048 m, 1968 vs, 1962 vs cm^{-1}. ^{1}H NMR (500 MHz, $CDCl_3$, 25 °C): δ 1.52 (t, 3H, CH_3, $^3J_{HH}$ = 7 Hz), 4.57 (q, 2H, CH_2, $^3J_{HH}$ = 7 Hz), 7.70 (d, 2H, $H^{5,7}$, $^3J_{HH}$ = 11 Hz), 9.78 (d, 2H, $H^{4,8}$, $^3J_{HH}$ = 11 Hz). ^{13}C{^{1}H} NMR (125 MHz, $CDCl_3$, 25 °C): δ 14.9 (*C*H_3), 61.5 (*C*H_2), 115.0, 129.6, 132.4, 137.5, 138.9, 141.0 (azulenic C), 161.1 (6-*C*N), 163.0 (*C*O_2Et), 165.9 (2-*C*N), 193.4 (W*C*O, *cis*), 194.0 (W*C*O, *cis*), 195.0 (W*C*O, *trans*), 196.2 (W*C*O, *trans*) ppm.

Synthesis and Separation of 8a and 9a. $Cr(CO)_5$(THF) was generated in situ by photolysis of $Cr(CO)_6$ (0.319 g, 1.45 mmol) dissolved in 500 mL of THF using a Hanovia Hg 450 W immersion lamp. After the formation of $Cr(CO)_5$(THF) had been judged nearly complete by FTIR in the ν_{CO} region, the resulting orange solution was added to a lavender solution of **6** (0.933 g, 2.89 mmol) in 20 mL of THF dropwise via cannula at room temperature. The mixture was stirred for 5 h, while slowly acquiring dark purple color. Then, the content of the flask was open to air, and all solvent was removed under vacuum on a rotary evaporator. The residue was chromatographed on silica gel using neat CH_2Cl_2 to elute four intensely colored bands that were separated and collected. Solvent removal from the first band (R_f = 0.79) afforded violet binuclear **7a** (0.158 g, 0.224 mmol) in a 31% yield

based on $Cr(CO)_6$ consumed. Solvent removal from the second (R_f = 0.53) and third (R_f = 0.39) bands provided blood red **8a** (0.223 g, 0.434 mmol) and **9a** (0.220 g, 0.428 mmol), respectively, both in 30% yields based on $Cr(CO)_6$ used. The final band proved to be unreacted **6**.

8a: blood red, decomposed without melting. Anal. Calcd for $C_{23}H_{14}CrN_2O_9$: C, 53.71; H, 2.74; N, 5.45. Found: C, 53.72; H 2.77; N, 5.52. IR (CH_2Cl_2): ν_{CN} 2135 w, 2115 w; ν_{CO} 2043 m, 1962 vs cm^{-1}. ^1H NMR (500 MHz, $CDCl_3$, 25 °C): δ 1.51 (t, 3H, CH_3, $^3J_{HH}$ = 7 Hz), 4.59 (q, 2H, CH_2, $^3J_{HH}$ = 7 Hz), 7.78 (d, 2H, $H^{5,7}$, $^3J_{HH}$ = 11 Hz), 9.78 (d, 2H, $H^{4,8}$, $^3J_{HH}$ = 11 Hz). $^{13}C\{^1H\}$ NMR (125 MHz, $CDCl_3$, 25 °C): δ 14.8 (*C*H_3), 61.6 (*C*H_2), 114.7, 129.4, 133.3, 135.8, 139.0, 141.5 (azulenic C), 163.0 (*C*O_2Et), 169.7 (6-*C*N), 186.6 (2-*C*N), 214.4 (Cr*C*O, *cis*), 216.3 (Cr*C*O, *trans*) ppm.

9a: blood red, decomposed without melting. Anal. Calcd for $C_{23}H_{14}CrN_2O_9$: C, 53.71; H, 2.74; N, 5.45. Found: C, 54.24; H 2.73; N, 5.34. IR (CH_2Cl_2): ν_{CN} 2125 br w; ν_{CO} 2033 m, 1965 vs cm^{-1}. ^1H NMR (500 MHz, $CDCl_3$, 25 °C): δ 1.52 (t, 3H, CH_3, $^3J_{HH}$ = 7 Hz), 4.57 (q, 2H, CH_2, $^3J_{HH}$ = 7 Hz), 7.70 (d, 2H, $H^{5,7}$, $^3J_{HH}$ = 11 Hz), 9.76 (d, 2H, $H^{4,8}$, $^3J_{HH}$ = 11 Hz). $^{13}C\{^1H\}$ NMR (125 MHz, $CDCl_3$, 25 °C): δ 14.5 (*C*H_3), 61.6 (*C*H_2), 114.8, 129.0, 131.7, 138.2, 139.7, 140.2 (azulenic C), 163.1 (*C*O_2Et), 179.3 (2-*C*N), 182.0 (6-C*N*), 214.1 (Cr*C*O, *cis*), 215.3 (Cr*C*O, *trans*) ppm.

Synthesis and Separation of 8b and 9b. Substitution of $W(CO)_6$ for $Cr(CO)_6$ in the above procedure for the synthesis of **8a** and **9a** afforded **7b**, **8b**, and **9b** in a 1.0:2.1:1.2 ratio.

8b: red−orange, decomposed without melting. Anal. Calcd for $C_{23}H_{14}N_2O_9W$: C, 42.75; H, 2.18; N, 4.34. Found: C, 43.08; H 2.02; N, 4.44. IR (CH_2Cl_2): ν_{CN} 2135 w, 2114 w; ν_{CO} 2043 m, 1955 vs cm^{-1}. ^1H NMR (500 MHz, $CDCl_3$, 25 °C): δ 1.52 (t, 3H, CH_3, $^3J_{HH}$ = 7 Hz), 4.58 (q, 2H, CH_2, $^3J_{HH}$ = 7 Hz), 7.78 (d, 2H, $H^{5,7}$, $^3J_{HH}$ = 11 Hz), 9.81 (d, 2H, $H^{4,8}$, $^3J_{HH}$ = 11 Hz). $^{13}C\{^1H\}$ NMR (125 MHz, $CDCl_3$, 25 °C): δ 14.9 (*C*H_3), 61.6 (*C*H_2), 115.0, 129.5, 133.3, 136.0, 139.1, 141.5 (azulenic C), 162.9 (*C*O_2Et), 165.9 (2-*C*N), 169.9 (6-*C*N), 194.0 (W*C*O, *cis*), 196.1 (W*C*O, *trans*) ppm.

9b: red−orange, decomposed without melting. Anal. Calcd for $C_{23}H_{14}N_2O_9W$: C, 42.75; H, 2.18; N, 4.34. Found: C, 43.15; H 2.18; N, 4.07. IR (CH_2Cl_2): ν_{CN} 2124 br w; ν_{CO} 2031 m, 1961 vs cm^{-1}. ^1H NMR (500 MHz, $CDCl_3$, 25 °C): δ 1.52 (t, 3H, CH_3, $^3J_{HH}$ = 7 Hz), 4.54 (q, 2H, CH_2, $^3J_{HH}$ = 7 Hz), 7.72 (d, 2H, $H^{5,7}$, $^3J_{HH}$ = 11 Hz), 9.78 (d, 2H, $H^{4,8}$, $^3J_{HH}$ = 11 Hz). $^{13}C\{^1H\}$ NMR (125 MHz, $CDCl_3$, 25 °C): δ 14.4 (*C*H_3), 61.7 (*C*H_2), 114.9, 129.2, 131.9, 138.2, 139.7, 140.3 (azulenic C), 161.4 (6-*C*N),163.1 (*C*O_2Et), 179.5 (2-*C*N), 193.3 (W*C*O, *cis*), 195.0 (W*C*O, *trans*) ppm.

Synthesis of 10. The use of dry reagents, solvents, and glassware is imperative for reproducibility of this reaction. A solution of phosphorus oxychloride (0.082 g, 0.050 mL, 0.534 mmol) in 10 mL of CH_2Cl_2 was added to a solution of **5** (0.180 g, 0.502 mmol) and diisopropylamine (1 mL, ca. 13 mmol) in 60 mL of CH_2Cl_2 under argon at 0 °C over the course of 1 h. The reaction mixture was stirred for 30 min after the addition of $POCl_3$ had been completed and then quenched with 100 mL of 10% aqueous $KHCO_3$. The organic layer was separated and dried over anhydrous Na_2SO_4. Filtration followed by removal of all volatiles at $T \leq 32$ °C afforded a dark red residue, which was subject to column chromatography on silica gel using neat $CHCl_3$. A salmon-colored band was collected, which gave crystalline **10** (0.118 g, 0.347 mmol) in a 70% yield after solvent removal and drying at 10^{-2} Torr. Mp 137−139 °C. Anal. Calcd for $C_{18}H_{16}N_2O_5$: C, 63.52; H, 4.74; N, 8.23. Found: C, 63.48; H 4.67; N, 8.03. IR (CH_2Cl_2): ν_{NH} 3286 br w; ν_{CN} 2116 s, 1710 m, 1693 m, 1666 w cm^{-1}. ^1H NMR (400 MHz, $CDCl_3$, 25 °C): δ 1.47 (t, 3H, CH_3, $^3J_{HH}$ = 7 Hz), 4.50 (q, 2H, CH_2, $^3J_{HH}$ = 7 Hz), 7.62 (d, 2H, $H^{5,7}$, $^3J_{HH}$ = 11 Hz), 8.66 (d, 1H, C*H*O, $^3J_{HH}$ < 2 Hz), 9.29 (d, 2H, $H^{4,8}$, $^3J_{HH}$ = 11 Hz), 10.45 (s br, 1H, N*H*) ppm. $^{13}C\{^1H\}$ NMR (100.6 MHz, $CDCl_3$, 25 °C): δ 14.5 (*C*H_3), 61.5 (*C*H_2), 128.7, 132.8, 134.8, 141.6 (azulenic C), 163.1 (br, *C*HO), 165.2 (*C*O_2Et), 167.7 (6-*C*N) ppm. Increasing solvent polarity (20% ethanol) eluted crude unreacted **5** (0.064 g, 0.179 mmol).

Synthesis of 11. $Cr(CO)_5$(THF) was generated in situ by photolysis of $Cr(CO)_6$ (0.071 g, 0.323 mmol) dissolved in 60 mL of THF using a Hanovia Hg 450 W immersion lamp. After the formation of $Cr(CO)_5$-(THF) had been judged nearly complete by FTIR in the ν_{CO} region, the resulting orange solution was added to a salmon-colored solution of **10** (0.100 g, 0.294 mmol) in 20 mL of THF dropwise via cannula at room temperature. The mixture was stirred for 4 h. Then, the content of the flask was open to air, and all solvent was removed under vacuum on a rotary evaporator. The product was passed through a short silica gel column using the 1:4 EtOAc/hexanes eluent. An orange band was collected. After solvent removal and drying at 10^{-2} Torr, deep orange crystalline **11** (0.137 g, 0.257 mmol) was isolated in an 87% yield. Mp 160−164 °C (dec). Anal. Calcd for $C_{23}H_{16}CrN_2O_{10}$: C, 51.89; H, 3.03; N, 5.26. Found: C, 51.21; H 2.85; N, 5.00. The value of %C proved somewhat low upon re-analysis. IR (CH_2Cl_2): ν_{CN} 2125 w; ν_{CO} 2040 m, 1962 vs, 1709 m, 1668 w cm^{-1}. ^1H NMR (500 MHz, $CDCl_3$, 25 °C, Figure S2): δ 1.47 (t, 3H, CH_3, $^3J_{HH}$ = 7 Hz), 4.50 (q, 2H, CH_2, $^3J_{HH}$ = 7 Hz), 7.63 (d, 2H, $H^{5,7}$, $^3J_{HH}$ = 10 Hz), 8.66 (s, 1H, C*H*O, $^3J_{HH} \approx 0$ Hz), 9.30 (d, 2H, $H^{4,8}$, $^3J_{HH}$ = 10 Hz), 10.43 (s, br, 1H, N*H*) ppm. $^{13}C\{^1H\}$ NMR (125 MHz, $CDCl_3$, 25 °C, Figure S3): δ 14.6 (*C*H_3), 61.5 (*C*H_2), 128.5, 134.4, 134.9, 140.2, 141.5 (azulenic C), 161.8 (br, *C*HO), 165.3 (*C*O_2Et), 178.3 (Cr*C*N), 214.1 (Cr*C*O, *cis*), 215.8 (Cr*C*O, *trans*) ppm.

Synthesis of 9a from 11. Phosphorus oxychloride (0.038 mL, 0.406 mmol) was added to a cooled (0 °C) solution of **11** (0.200 g, 0.376 mmol) and diisopropylamine (0.26 mL, 1.8 mmol) in 25 mL of CH_2Cl_2. The mixture was stirred for 3 h while warming up to room temperature. Then, the content of the flask was open to air and washed with 25 mL of 10% Na_2CO_3. The organic layer was washed with 2 × 50 mL of water and dried over anhydrous Na_2SO_4. The resulting mixture was filtered, and all volatiles were removed under vacuum on a rotary evaporator. The crude product was passed through a short plug of silica gel using the 1:2 EtOAc/hexanes eluent. A blood red band was collected which gave crystalline **9a** (0.175 g, 0.340 mmol) in a 90% yield after solvent removal and drying at 10^{-2} Torr. The product was spectroscopically (IR, ^1H, and ^{13}C NMR) identical to bona fide **9a** described above.

Synthesis of 12a. $W(CO)_5$(THF) was generated in situ by photolysis of $W(CO)_6$ (0.087 g, 0.247 mmol) dissolved in 65 mL of THF using a Hanovia Hg 450 W immersion lamp. After the formation of $W(CO)_5$-(THF) had been judged nearly complete (FTIR), the resulting yellow−orange solution was added to a blood red solution of **9a** (0.115 g, 0.224 mmol) in 15 mL of THF dropwise via cannula at room temperature. The mixture was stirred for 2.5 h. Then, all solvent was removed under vacuum. The product was subject to chromatography on a short silica gel column using the 1:1 CH_2Cl_2/hexanes eluent. A dark magenta band was collected. After solvent removal and drying at 10^{-2} Torr, very dark magenta (almost black) **12a** (0.159 g, 0.190 mmol) was isolated in an 85% yield. Mp 191−195 °C (dec). Anal. Calcd for $C_{28}H_{14}CrN_2O_{14}W$: C, 40.12; H, 1.68; N, 3.34. Found: C, 40.23; H 1.69; N, 3.30. IR (CH_2Cl_2): ν_{CN} 2135 w, 2123 w; ν_{CO} 2026 m, 1962 vs cm^{-1}. ^1H NMR (500 MHz, $CDCl_3$, 25 °C): δ 1.52 (t, 3H, CH_3, $^3J_{HH}$ = 7 Hz), 4.58 (q, 2H, CH_2, $^3J_{HH}$ = 7 Hz), 7.69 (d, 2H, $H^{5,7}$, $^3J_{HH}$ = 11 Hz), 9.78 (d, 2H, $H^{4,8}$, $^3J_{HH}$ = 11 Hz) ppm. $^{13}C\{^1H\}$ NMR (125 MHz, $CDCl_3$, 25 °C): δ 14.9 (*C*H_3), 61.5 (*C*H_2), 114.9, 129.3, 132.4, 137.6, 139.0, 140.9 (azulenic C), 163.0 (*C*O_2Et), 165.8 (W*C*N), 181.8 (Cr*C*N), 194.0 (W*C*O, *cis*), 196.2 (W*C*O, *trans*), 213.8 (Cr*C*O, *cis*), 215.3 (Cr*C*O, *trans*) ppm.

Synthesis of 12b. Switching conditions (ii) and (iv) in Scheme 2 afforded **12b** in ca. 80% yield based on **10**. Mp 176−179 °C (dec). Anal. Calcd for $C_{28}H_{14}CrN_2O_{14}W$: C, 40.12; H, 1.68; N, 3.34. Found: C, 39.96; H 1.76; N, 3.37. IR (CH_2Cl_2): ν_{CN} 2133 w, 2125 w; ν_{CO} 2025 m, 1961 vs cm^{-1}. ^1H NMR (500 MHz, $CDCl_3$, 25 °C): δ 1.51 (t, 3H, CH_3, $^3J_{HH}$ = 7 Hz), 4.58 (q, 2H, CH_2, $^3J_{HH}$ = 7 Hz), 7.70 (d, 2H, $H^{5,7}$, $^3J_{HH}$ = 11 Hz), 9.75 (d, 2H, $H^{4,8}$, $^3J_{HH}$ =11 Hz) ppm. $^{13}C\{^1H\}$ NMR (125 MHz, $CDCl_3$, 25 °C): δ 14.8 (*C*H_3), 61.5 (*C*H_2), 114.7, 129.4, 132.6, 137.4, 138.8, 141.0 (azulenic C), 160.8 (W*C*N), 163.1

(CO_2Et), 186.0 (Cr*C*N), 193.4 (W*C*O, *cis*), 195.1 (W*C*O, *trans*), 214.4 (Cr*C*O, *cis*), 216.4 (Cr*C*O, *trans*) ppm.

X-ray Work. X-ray quality crystals of **7a**, **7b**, **8a**, **10**, **12a**, and **12b** were grown at 4 °C by layering pentane over CH_2Cl_2 solutions of the above complexes. Intensity data were collected using a Bruker APEX CCD area detector mounted on a Bruker D8 goniometer. Graphite-monochromated Mo Kα radiation ($\lambda = 0.71073$ Å) was employed. All structures were solved by direct methods and refined by full-matrix least-squares methods on F^2 using the SHELXTL V5.0 suite of programs. All data were corrected for absorption by a semi-empirical method.[42] A full description of the X-ray diffraction experiments is available in the Supporting Information.

DFT Calculations. Time-dependent density functional theory calculations were performed in Gaussian 98[43] via the random phase approximation extension to conventional Kohn−Sham density functional theory. The solid-state geometry of **7a** was considered in these calculations. Ten lowest lying excited states were resolved and characterized at the 6-31G(2df,2p) level[44,45] using the BLYP exchange correlation functional.[46,47] The three closely spaced (within 0.184 eV) lowest excited states for **7a** were determined to be: (1) HOMO-1 → LUMO, $f = 0.0003$; (2) HOMO-2 → LUMO, $f = 0.0003$; (3) (0.52 × HOMO + 0.29 × HOMO-3 − 0.31 × HOMO-4) → LUMO, $f = 0.2938$ (f = oscillator strength).

Acknowledgment. This work was funded by the National Science Foundation (CHE-0548212), Kansas Technology Enterprise Corporation, and the University of Kansas. The authors thank Dr. Douglas R. Powell for useful discussions pertaining to the X-ray work. E.M.W. gratefully acknowledges support by the NSF REU Site Grant CHE-0244041.

Supporting Information Available: Details of the X-ray diffraction work for **7a**, **7b**, **8a**, **10**, **12a**, and **12b**; electronic spectra of **6**, **12a**, and **12b**; ^{1}H and ^{13}C NMR spectra of **11**; complete refs 9d, 14a, 16b, and 43. This material is available free of charge via the Internet at http://pubs.acs.org.

JA053933+

(42) Sheldrick, G. M. *SADABS. Program for Empirical Absorption Correction of Area Detector Data*; University of Göttingen: Germany, 2000.
(43) Frisch, M. J.; et al. *Gaussian 98*, revision A.10; Gaussian, Inc.: Pittsburgh, PA, 1998.
(44) Ditchfield, R.; Hehre, W. J.; Pople, J. A. *J. Chem. Phys.* **1971**, *54*, 724−728.
(45) Frisch, M. J.; Pople, J. A.; Binkley, J. S. *J. Chem. Phys*. **1984**, *80*, 3265−3269.
(46) Lee, C.; Yang, W.; Parr, R. G. *Phys. Rev. B* **1988**, *37*, 785−789.
(47) Becke, A. D. *J. Chem. Phys.* **1996**, *104*, 1040−1046.